Vibration Analysis of a Loudspeaker via Michelson Interferometer

Hacı Berkay Buz[1,*]

[1] *Department of Physics, Bilkent University, Ankara 06800, Türkiye*

(Dated: December 26, 2025)

The Michelson Interferometer, invented by A. A. Michelson in 1880, was famously used in the Michelson-Morley experiment in 1887. It has since been applied in many areas of science due to its ability to measure tiny motions. In this experiment, a modified interferometer setup was used to analyze loudspeaker vibrations. One mirror was mounted on the loudspeaker, causing the interference pattern to change as it oscillated. These changes were captured by a photodetector and analyzed using Fast Fourier Transform (FFT). The vibration frequencies were measured with a relative error of approximately 0.1%. Additionally, harmonic distortion caused by the loudspeaker was successfully detected. Finally, complex audio signals, such as music, were reconstructed from the interference data, which demonstrates the high sensitivity of the system.

INTRODUCTION

Throughout human history, optics has been a fundamental area of physics that has attracted interest. In the late 19th century, Albert A. Michelson, a successful physicist, played a significant role in the development of this field. He performed several experiments on the speed of light and successfully measured it in 1879 by using the method of the rotating mirror [1]. Then, in 1887, together with Edward W. Morley, he carried out his famous experiment using Michelson interferometer, which disproved the aether. This showed that light travels at the same speed in all inertial systems, contrary to their original hypothesis [1].

The Michelson interferometer is regarded as a fundamental instrument in wave optics. It operates by splitting a light beam into two paths and recombining them. This process produces interference fringes that are highly sensitive to small changes in the optical path. Due to this sensitivity, these interferometers are utilized in modern optical research. For instance, measurements such as the coherence length of lasers are enabled by this device [2]. Furthermore, contemporary versions play a key role in the detection of gravitational waves, where extremely small length variations are monitored [3].

In this project, the high sensitivity of the Michelson interferometer to small displacements was investigated. A loudspeaker was utilized to provide a controlled source of vibration. To reflect the laser beam, a mirror was attached to the surface of the loudspeaker. As the loudspeaker created sound, the mirror oscillated. This movement caused tiny changes in the optical path length. As a result, the interference fringes were shifted. These shifts were recorded as changes in light intensity. By analyzing this data, the vibration frequencies were measured with high precision. Additionally, the full vibration signal was reconstructed from the light intensity data. These demonstrate the effectiveness of optical interferometry for vibration analysis.

THEORY

Michelson Interferometer

A Michelson interferometer consists of a beam splitter, two planar mirrors, and a monochromatic laser. In the standard setup, a compensating plate is also used [2], but it is not needed in this experiment because we use a monochromatic laser.

The laser light splits into two beams at the beam splitter. Each beam is reflected by a mirror and returns to the beam splitter, where they meet and interfere. If the two beams travel different distances, a phase difference occurs. This determines whether the interference is constructive or destructive.

Constructive interference occurs when the path difference satisfies:

$$\Delta d = d_2 - d_1 = n\frac{\lambda}{2} \tag{1}$$

where d_1 and d_2 are the distances from the beam splitter to the mirrors, λ is the wavelength of the light, and n is an arbitrary integer [4].

Two partial light beams can be represented as:

$$E_1 = Ae^{i(\omega t+\phi_1)}$$
$$E_2 = Ae^{i(\omega t+\phi_2)}$$

where A is the amplitude, t is time, ϕ_1 and ϕ_2 are phases and ω is the frequency. Therefore, the resultant wave:

$$E = E_1 + E_2 = Ae^{i\omega t}(e^{i\phi_1} + e^{i\phi_2})$$

The squared magnitude is:

$$|E|^2 = EE^*$$
$$|E|^2 = Ae^{i\omega t}(e^{i\phi_1} + e^{i\phi_2}) \times Ae^{-i\omega t}(e^{-i\phi_1} + e^{-i\phi_2})$$
$$|E|^2 = A^2\left[e^0 + e^{i(\phi_1-\phi_2)} + e^{i(\phi_2-\phi_1)} + e^0\right]$$
$$|E|^2 = 2A^2(1 + \cos(\Delta\phi))$$

where $\Delta\phi = \phi_1 - \phi_2$. From the Equation 1, this equation can be written as:

$$|E|^2 = 2A^2(1 + \cos(2\pi\frac{2\Delta d}{\lambda})) \tag{2}$$

Since the response of the photodiode is proportional to the magnitude of the light waves, this equation will help to estimate the relative response of the photo detector [5].

One of the mirrors is fixed, while the other is attached to a loudspeaker. The loudspeaker makes the mirror in front of it vibrate, which changes the optical path difference, $d_2 - d_1$. The loudspeaker produces oscillations at a fixed frequency, which can be described as:

$$L \approx A_1 \sin(\omega t) \tag{3}$$

where A_1 is the amplitude of the vibration, corresponding to the mirror's displacement, and ω is the angular frequency.

These oscillations cause the interference fringes to move, producing harmonic changes in the output current of the photodetector [6]. From Equations 2 and 3, the light intensity, and therefore the photodetector response, can be expressed as:

$$|E|^2 = 2A^2\left(1 + \cos\left(2\pi\frac{2\sin(\omega t)}{\lambda}\right)\right) \tag{4}$$

This time-varying signal will be recorded and analyzed on Python using Fast Fourier Transform Algorithm.

Fast Fourier Transform (FFT)

The mirror displacement is caused by the vibration of the loudspeaker. This changes the light intensity measured by the photodetector. Consequently, a time-domain signal containing the vibration frequency information is produced.

Fourier analysis is used to find the frequency components of this signal. For a signal $x[n]$ with N data points, the Discrete Fourier Transform (DFT) is defined as

$$X[k] = \sum_{n=0}^{N-1} x[n]\, e^{-i2\pi kn/N}, \tag{5}$$

where k represents the frequency index. The magnitude $|X[k]|$ shows the strength of each frequency component.

Direct calculation of the DFT is slow. Instead, the Fast Fourier Transform (FFT) algorithm is used. While it produces the same result, the operation of this algorithm is involved and difficult to explain in detail. However, it is preferred because it is much more efficient for analyzing large datasets [7].

In this experiment, the FFT was applied to the photodetector signal to find the dominant vibration frequencies. The peaks in the frequency spectrum correspond to the driving frequency and its harmonics. This allows the vibration and any harmonic distortion to be measured precisely.

Lens Magnification

A diverging lens is used to make the laser beam pattern seem larger on the observation plane. The magnification of the lens can be found from geometrical optics:

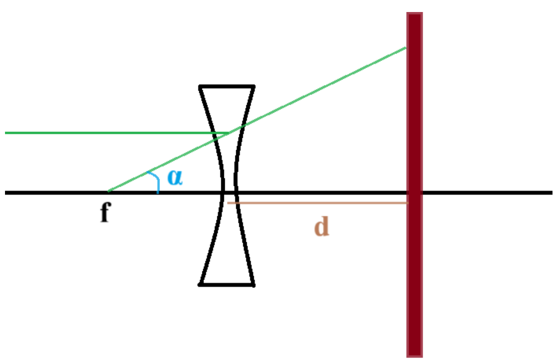

FIG. 1. Illustration of magnification produced by a diverging lens. Here, f is the focal length, d is the distance between the lens and the observation plane, and α is the angle of the refracted ray.

Let the distance between the lens and the observation plane be denoted by d, and let f be the focal length of the lens. As shown in Fig. 1, the incoming ray leaves the lens at an angle α. Using similar triangles, the height of the beam before the lens (y) and the height of the beam on the observation plane (y') can be related.

$$\tan\alpha = \frac{y}{f} = \frac{y'}{f+d} \tag{6}$$

This relation directly gives the magnification produced by the lens:

$$M = \frac{y'}{y} = \frac{f+d}{f} \tag{7}$$

This formula shows how the magnification depends on the lens position and on its focal length. Using this expression, the correct place for the lens can be chosen to get the desired size of the interference pattern on the observation plane [8].

METHODOLOGY

The experimental setup includes a 532 nm green laser as the light source, a beam splitter, two mirrors, and a loudspeaker that will act as the source of vibration. The photodetector consists of photodiodes with an amplification circuit, connected to a PC for data acquisition and analysis

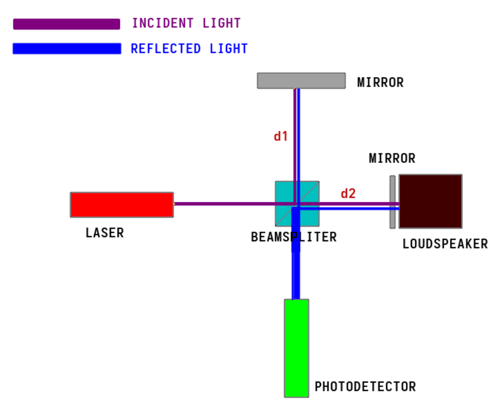

FIG. 2. A schematic illustration of the setup, consisting of a laser, beam splitter, loudspeaker, two mirrors, and a photodetector.

1. First, the experimental environment was prepared. Direct contact with the ground

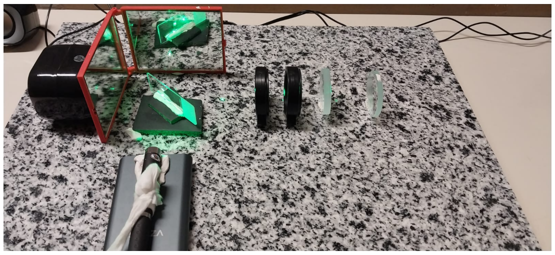

FIG. 3. An image of the final experimental setup. Laser beam, loudspeaker, microscope lamella (as a beam splitter), mirrors and lenses are shown in the figure.

was avoided because vibrations could affect the measurements. To solve this, contact was minimized using seismic isolators, and a heavy granite marble was placed on top to reduce vibration and create a flat surface.

2. A microscope slide was positioned on the surface to act as a beam splitter. The separated beams were reflected by mirrors and recombined at the slide. Foldable mirrors were used because separate mirrors were found to be very susceptible to ambient vibrations. It is believed that these interconnected mirrors improve stability Because they vibrate together when exposed to external disturbances and this does not make change in the optical path difference.

3. The recombined beam was directed toward the photodiode. However, since the beam was initially small, the pattern was magnified using diverging lenses according to the Equation 7. A dark fringe was aligned to fall directly on the photodiode. In this way, the constant signal was minimized. This made the vibrations in the pattern more detectable by the sensor.

4. Next, a photodetector circuit was prepared using a BPW34S silicon PIN photodiode. This photodiode is suitable because it is sensitive to wavelengths between 420 nm and 1120 nm, which covers the 532 nm wavelength of the green laser. It also has a fast response time of approximately 20 ns, allowing detection of rapid changes in the interference pattern caused by the loudspeaker vibrations [9]. The signal was amplified using a TLV2462 op-amp and a 1 MΩ resistor. Additionally, a 100 nF capacitor was included to minimize high-frequency noise and ensure a stable signal. Finally, the data was transferred from the Arduino to the computer.

5. The light intensity was monitored using Python, where changes in the interference pattern were used to determine the vibration frequency of the loudspeaker. The recorded data was then processed using Fast Fourier Transform (FFT) tools in Python to analyze the frequency components.

6. The frequency obtained from the FFT was compared with the original input frequency sent to the loudspeaker. As a final step, the recorded vibration signal was converted back into sound. This provided a simple way to verify that the system was working correctly and that the recorded signal matched the original input.

RESULTS

The interference pattern obtained from the interferometer is shown in Figure 4. At first, the pattern was too small to be observed clearly with the naked eye. Therefore, a lens system was used to magnify the pattern. In this way, the interference fringes became clearly visible.

Initially, the setup was sensitive to external disturbances, such as walking nearby or environmental noise. However, by using isolators to minimize these vibrations, the signal was successfully recorded.

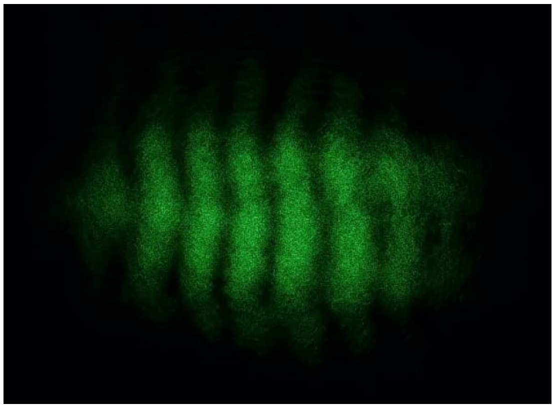

FIG. 4. Magnified image of the interference pattern. Fringes are clearly well defined and visible.

The experiment is started with single frequencies. The results for the 400 Hz sound are shown in Figure 5. The primary frequency was clearly 400 Hz. Integer multiples, such as 800 Hz, were also detected due to harmonic distortion.

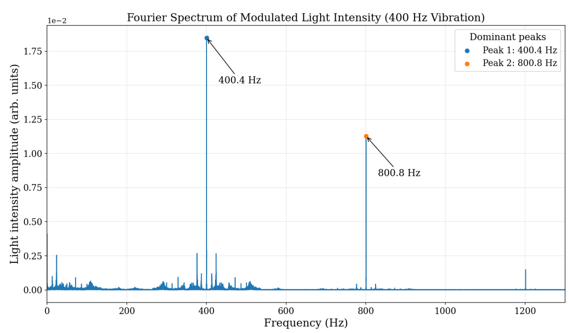

FIG. 5. The frequency spectrum with only 400 Hz sound. The peak is very sharp and this shows the precision of the setup for vibration analysis.

Harmonic distortion is caused because the loudspeaker is not perfectly linear. Ideally, only the main frequency should be produced. However, perfectly linear movement is not achieved by real loudspeakers. Because of this, extra peaks are created at multiples of the original frequency. These are called harmonics which explains the extra peaks found in the data [10]. The accuracy was determined by comparing the measured peak to the input frequency. A relative error of about 10^{-3} was calculated. This indicates that low-frequency vibrations were detected with high precision. The sharp peak also suggests good frequency resolution, which was limited mainly by sampling time and noise. After measuring this single frequency accurately, a superposition of two different waves is sent from the loudspeaker. The frequencies obtained for 400 Hz and 600 Hz are shown in Figure 6.

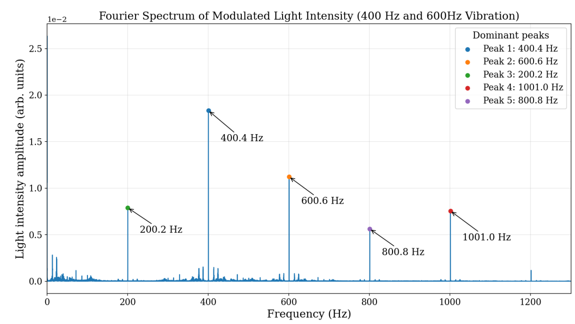

FIG. 6. Frequency spectrum of the 400 Hz and 600 Hz. The dominating peaks are those two. However, due to harmonic distortion, linear combinations like 200 Hz or 800 Hz are also visible in the spectrum.

Again, the highest peaks are the frequencies that were sent. However, linear combinations of these two frequencies are visible because of harmonic distortion. Nevertheless, the precision of the obtained signals is surprisingly good. Finally, we tried sending 3 signals together: 400 Hz, 600 Hz, and 1000 Hz. The obtained frequency distribution is shown in Figure 7.

A 1000 Hz frequency was also observed during the $400-600$ Hz test. This was formed by the combination of the other frequencies. However, in the $400-600-1000$ Hz case, an actual 1000 Hz signal was added to the input. As a result, the size of the 1000 Hz peak was increased, making it the third dominant frequency. The relative errors for these frequencies are presented in Table I.

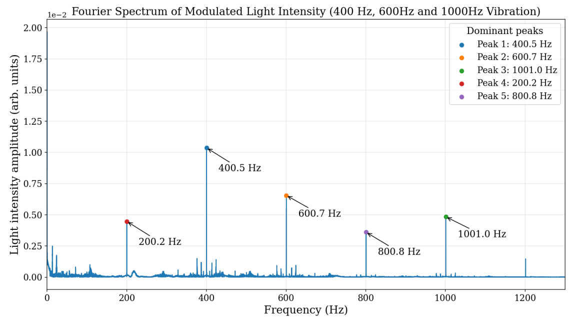

FIG. 7. Frequency spectrum of the 400 Hz, 600 Hz, and 1000 Hz vibrations. The results are very precise. But due to harmonic distortion, linear combinations of those results are also visible in the spectrum.

Frequency (Hz)	**Error (%)**
400	0.13
600	0.12
1000	0.10

TABLE I. Relative error between sent and measured frequencies obtained from the Fourier analysis.

The results were found to be precise. Even though harmonic distortion was present, the main frequencies were clearly identified. The frequency error was calculated to be around 0.1%, which indicates good performance for low frequencies. However, when high frequencies (50 Hz, 2000 Hz, and 5000 Hz) were applied together, the low frequencies dominated the signal. The high frequencies were barely detectable, as shown in Figure 8. This occurs because the physical vibration amplitude is typically much smaller at higher frequencies. This makes them harder to detect compared to the larger movements at low frequencies.

This indicates that the setup is less effective for high frequencies. Typically, low frequency sounds (bass) produce larger physical vibrations, which can overshadow the smaller vibrations caused by high-pitched sounds. Consequently, reconstructing the complex audio of

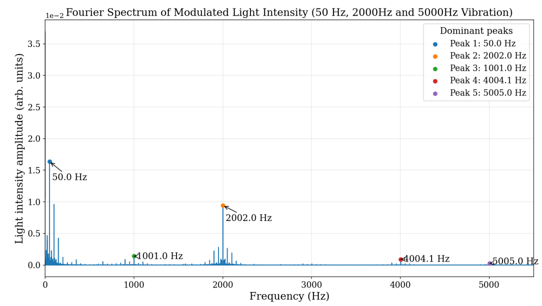

FIG. 8. Frequency spectrum of the 50 Hz, 2000 Hz, and 5000 Hz vibrations. Note that the precision is pretty good. However, even though the amplitudes of the sent frequencies are the same, their amplitude is not the same on the graph. This shows the inability of our setup to detect high-pitched sounds with the correct amplitude.

music from the vibration data was difficult. However, recognizable sound was still obtained. A comparison between the original music and the reconstructed audio is shown in Figure 9.

Correlations with the actual sound were found in the $500 - 800$ Hz and $1100 - 1400$ Hz ranges, with a smaller match at $100 - 300$ Hz. However, significant differences were observed around $0 - 50$ Hz, and sharp, unexpected peaks appeared at 400 Hz and 1600 Hz. These anomalies confirm that the frequency spectrum was affected by harmonic distortion and background noise. Nevertheless, when the data was converted back into audio, the original sound was recognizable, despite some background static similar to radio noise. This successful reconversion of the audio and small errors in frequency measurements demonstrate the overall success of the experiment.

ERROR ANALYSIS

A major source of error was background vibration. Although isolators and a heavy granite table is used to minimize vibrations, the setup still picked up vibrations from movement in the

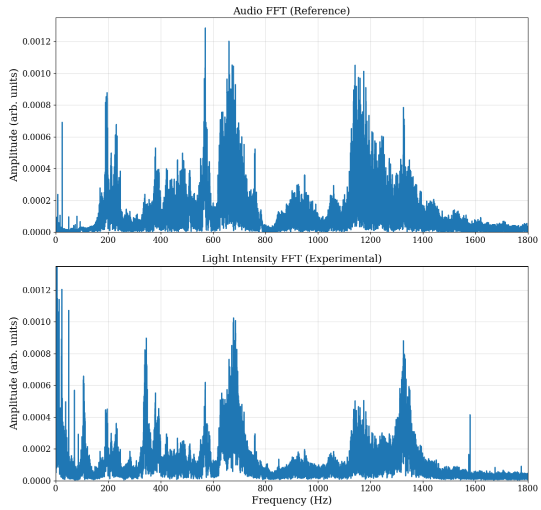

FIG. 9. Frequency spectrum of the sample audio and the light intensity spectrum of the obtained vibration data from the photodiode. There are some very good correspondences which allows to the music be heard, whereas there are some meaningless peaks due to harmonic distortion.

room. Future experiments would require better isolation equipment or a room specifically designed to block vibrations.

Additionally, the uneven quality of the laser beam reduced the accuracy of the study. The beam was not perfectly round or uniform, even before interference occurred. Because of this, the fringe spacing could not be measured correctly. To fix this, a laser with a smooth, uniform beam like He-Ne laser can be used.

The mirrors were mounted too close together, creating a mechanical connection. While this connection helped cancel out background vibrations, it also caused the reference mirror to move when the target mirror was driven. We reduced this error by lowering the sound level, but physically isolating the mirrors would prevent this effect entirely.

Finally, significant noise was observed in the output sound due to harmonic distortion. This is clearly shown in Figure 9. As seen in Figure 7, unwanted peaks were generated even with just three frequencies. Since music contains many frequencies at once, this noise was greatly increased. The main cause was the low quality of the loudspeaker used. If a high fidelity speaker is used, the distortion will be minimized. This would result in a much clearer sound.

CONCLUSION

This experiment aimed to analyze mirror vibration caused by sound by using the Michelson interferometer's ability to measure small distance changes. First, the setup was designed to minimize the external vibrations. This resulted in a stable interference pattern. Changes in the interference pattern caused by the sound were then observed. When a specific single frequency sound was sent, the transmitted frequency was recovered with approximately 0.1% error. This demonstrated the setup's sensitivity to small oscillations. Additionally, when multiple frequencies were sent simultaneously, linear combinations of these frequencies were obtained. This is due to harmonic distortion caused by the nonlinear nature of the speaker. However, the detection of this distortion demonstrates the success of the interferometer. Furthermore, the dominant frequencies matched the input frequencies again with a small error of around 0.1%. Finally, instead of specific frequencies, a music track was sent. Due to ambient noise and the amplification of distortion from sending many frequencies, the data obtained did not perfectly match the transmitted data. Nevertheless, when this data was converted back to sound, it was easily understandable despite some background noise. All this demonstrates that the Michelson interferometer is sensitive to small distance changes and can be used for vibration analysis.

* berkay.buz@ug.bilkent.edu.tr

[1] A. Lucas, *Albert A. Michelson and his Interferometer: Lord of the Spinning Worlds, Master of Light* (Cambridge Scholars Publishing, 2023) pp. 6–22.

[2] P. Hariharan, *Optical Interferometry*, 2nd ed. (Academic Press, 2003) Chap. 1.

[3] C. Bond, D. Brown, A. Freise, and K. A. Strain, Interferometer techniques for gravitational-wave detection, Living Reviews in Relativity **19**, pp. 43 to 56 (2016).

[4] F. A. Jenkins and H. E.White, *Fundamentals of Optics* (McGraw-Hill, 1976) pp. 271–276.

[5] J. Crawford, Frank S., Introduction and superposition of harmonic waves, in *Waves: Berkeley Physics Course, Volume 3* (McGraw-Hill, New York, 1968) pp. 403–495.

[6] J. Baker, R. Laming, T. Wilmshurst, and N. Halliwell, A new, high sensitivity laser vibrometer, Optics Laser Technology **22**, 241 (1990).

[7] A. L. Garcia, *Numerical Methods for Physics* (Prentice Hall, Englewood Cliffs, NJ, 2000) Chap. 5.2, pp. 153–162.

[8] E. Hecht, *Optics*, 5th ed. (Pearson Education, Boston, 2017) pp. 166–170.

[9] OSRAM Opto Semiconductors, BPW 34 S Silicon PIN Photodiode, `https://look.ams-osram.com/m/1f206a499ac1f0b2/original/BPW-34-S.pdf` (2021), datasheet, Version 1.7, Accessed: 2024-10-27.

[10] R. P. Feynman, R. B. Leighton, and M. Sands, *The Feynman Lectures on Physics*, Vol. I (Addison-Wesley, Reading, Massachusetts, 1964) Chap. 50.

GANTT CHART & TASK MANAGEMENT

Gantt Chart

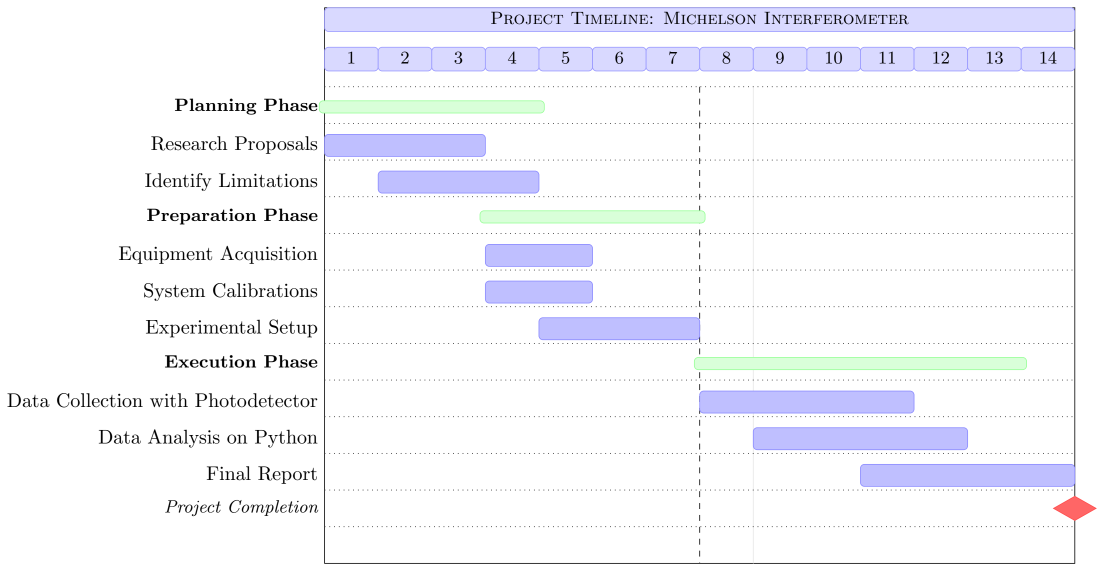

Task Assignments & Responsibilities

Task	Members	Weeks
Research Proposals	All Members	2–3
Identify Limitations	All Members	2–4
Equipment Acquisition	Berkay, Asrın	4–5
System Calibrations	All Members	4.5–5
Experimental Setup	Berkay, Asrın	5–7
Data Collection	All Members	8–11
Data Analysis/ Coding	Kayra, Berkay	9–12
Final Report	All Members	11–14
Project Completion	All Members	14